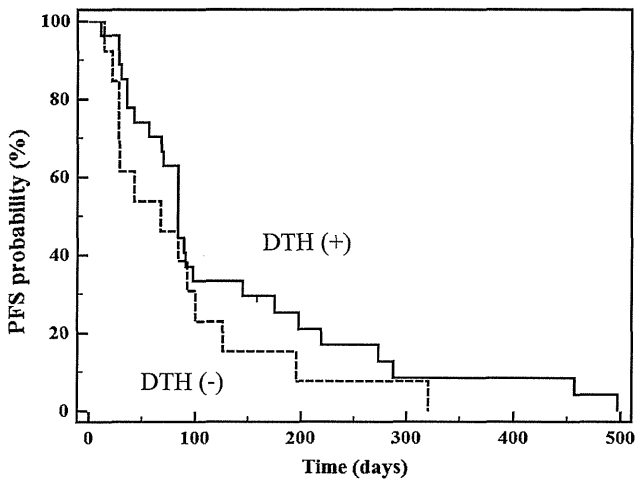

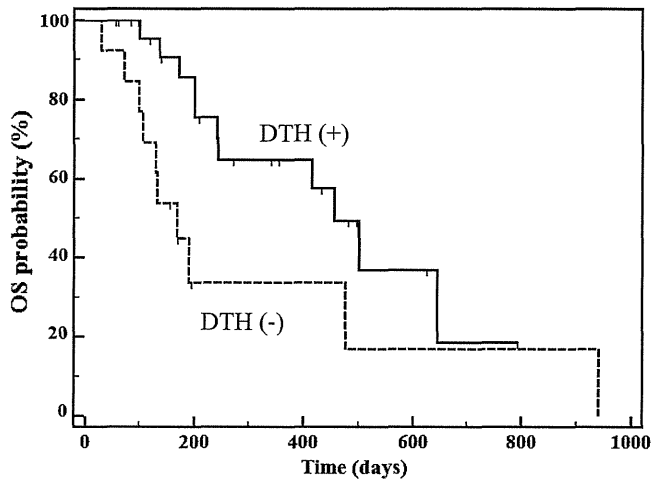

Fig. 1 PFS and OS association with DTH after WT1 vaccination. **a** The PFS tended to be longer in positive DTH cases than in DTH-negative cases ($p = 0.23$ by the log-rank test). **b** The OS was significantly longer in positive DTH cases than in DTH-negative cases ($p = 0.023$ by the log-rank test). *Solid line*: DTH (*plus*), *broken line*: DTH (*minus*)

Izumoto et al. 2008; Ohno et al. 2009). In this current phase II trial, we have tested the efficacy and safety of WT1 immunotherapy for gynecologic malignancies that were progressing, that is, resistant against conventional therapies.

In general, gynecologic tumors, including ovarian, endometrial and cervical carcinomas and uterine sarcomas, are very difficult to further treat, once the disease become resistant to conventional therapies such as chemotherapy or radiotherapy. For example, when ovarian carcinoma is first treated with cytoreductive surgery, the surgery is immediately followed by combination chemotherapy with paclitaxel and carboplatin (TC). If there is a failure of this first-line treatment, a single drug or combination chemotherapy for the recurrent disease, chosen based on the patient's treatment-free interval, can still be performed effectively in some cases (Koensgen et al. 2008; Markman et al. 2003; Harries and Gore 2002; Dizon et al. 2003). However, even though some third-line regimens have been reported to be occasionally effective for second relapses of some of these advanced stage diseases (Vergote et al. 2009; Chiyoda et al. 2010); the efficacy of each attempt becomes progressively lower as the number of previous treatment failures increases.

In the present study, the median number of the previous treatment regimens was 3 (range 1–11 treatments). Since all of the patients in the present trial had exhibited resistance to previous therapies, normally supportive care would have been considered as the only remaining option for them; however, the experimental WT1 vaccination immunotherapy was offered to them as an alternative.

A previous small study showed that stable disease was achieved by WT vaccination in 3 (25 %) of 12 gynecologic malignancies (Ohno et al. 2009). However, that study was so small that a survival effect was not analyzed. The response rate (CR + PR/all) in our study was 0 % (0 of 40 cases). However, the disease control rate (CR + PR + SD/all), which corresponds to disease stabilization lasting at least 3 months from the start of the vaccination, was 40 % (16 of 40 cases). The median PFS was 84 days (11–497), and the median OS of all the patients was 193 days (29–941). Considering that these cases were resistant to various kinds of therapies, and the diseases were progressing prior to the vaccination, these results of disease control rate and PFS time may be favorable, and were consistent with results of the previous smaller study that suggested the therapeutic potential of WT1 vaccine for gynecologic malignancies. Furthermore, surprisingly, in these SD cases, whose tumors had continuously progressed against previous therapies during the median of 185 days of treatments (range 40–1,198 days), the disease was durably controlled, without significant progression of the disease, for the median of longer than 160 days (range 67–427 days) after starting the WT1 immunotherapy (Table 2), implying an improved survival effect of the WT1 peptide vaccine. The adverse effect by the WT1 peptide-based immunotherapy with the dosage and schedule adopted here was limited and largely tolerable.

We next investigated the association of DTH and the efficacy of the WT1 immunotherapy. The OS of the patients with a positive DTH reaction was significantly better than that of those with a negative DTH reaction ($p = 0.023$ by the log-rank test) (Fig. 1). Moreover, the DTH reaction was demonstrated to be an independent factor for overall survival of the patients by multivariate Cox proportional hazards analysis (Table 3). These findings suggested that the induction of WT1-specific immune response, that is, the peptide-specific DTH, is a potential

Table 3 Multivariate Cox proportional hazards analysis on overall survival

Variable	Number of cases	Adjusted HR	95 % CI	*p* value
Age (years)				0.44
<60	24	1		
≥60	16	0.64	0.21–1.96	
Origin of the disease				0.75
Uterus	16	1		
Ovary	24	1.17	0.44–3.14	
Histology				0.98
Carcinoma	35	1		
Sarcoma, carcinosarcoma	5	0.99	0.28–3.42	
Evaluation of the previous therapy				0.39
SD	4	1		
PD	36	1.88	0.46–7.71	
Number of previous therapy regimens				0.034
<3	12	1		
≥3	28	4.28	1.12–16.37	
DTH				0.043
+	27	1		
−	13	2.73	1.04–7.19	

Multivariate Cox proportional hazards analysis (stepwise method) for the factors including age, origin of the disease, histology, evaluation of the previous therapy, number of previous therapy regimens and DTH was performed to evaluate whether DTH was an independently significant factor on OS

SD stable disease, *PD* progressive disease

predictor for the induction of clinical response, leading to a better prognosis.

The number of previous treatment regimens was also demonstrated to be an independent factor for survival prognosis after WT1 immunotherapy. The response rate of the first-line chemotherapy was quite high for ovarian carcinoma, however, that of second-line and the third-line chemotherapy was 34.5 and 27.5 %, respectively (Nishio et al. 2006). Effectiveness of WT1 was demonstrated to be associated with the number of previous treatment regimens, which was similar to that of the cell toxic chemotherapy. As the number of chemotherapy regimen increases, the tumor cells are considered to become resistant to the next line therapy. Furthermore, immunological potentials of the patients treated by chemotherapy with many courses might be dampened, leading to the poor response to the administered cancer vaccine. WT1 peptide vaccination soon after the first-line therapy, including the vaccination to prevent relapse after the operation, chemotherapy or radiation therapy, may be a favorable setting for the next clinical trial.

In the present phase II prospective study with a single arm, we have, for the first time, analyzed the survival effect of the WT1 vaccine for gynecologic malignancies, in addition to its anti-tumor effect conventionally evaluated by RECIST and toxicity, which had previously been reported in a smaller pilot study (Ohno et al. 2009). It was strongly suggested that WT1 peptide vaccination could induce the peptide-specific immune response in patients whose gynecological tumors have become resistant to conventional therapies, leading to a better survival. Larger two-arm randomized studies will be required to confirm the efficacy and clinical usefulness of the WT1 peptide vaccine for gynecologic malignancies.

Acknowledgments We would like to thank Dr. G.S. Buzard, US CDCP, for his editing of our manuscript. We are also grateful to Ms. T. Umeda for her excellent technical assistance.

Conflict of interest The authors have no conflict of interest.

References

Cheever MA, Allison JP, Ferris AS, Finn OJ, Hastings BM, Hecht TT, Mellman I, Prindiville SA, Viner JL, Weiner LM, Matrisian LM (2009) The prioritization of cancer antigens: a National Cancer Institute pilot project for the acceleration of translational research. Clin Cancer Res 15:5323–5337

Chiyoda T, Tsuda H, Nomura H, Kataoka F, Tominaga E, Suzuki A, Susumu N, Aoki D (2010) Effects of third-line chemotherapy for women with recurrent ovarian cancer who received platinum/taxane regimens as first-line chemotherapy. Eur J Gynaecol Oncol 31:364–368

DiSaia PJ, Creasman WT (2002) Clinical gynecologic oncology, 6th edn. St Louis, Mosby

Dizon DS, Dupont J, Anderson S, Sabbatini P, Hummer A, Aghajanian C, Spriggs D (2003) Treatment of recurrent ovarian cancer: a retrospective analysis of women treated with single-agent carboplatin originally treated with carboplatin and paclitaxel. The memorial sloan-kettering cancer center experience. Gynecol Oncol 91:584–590

Dohi S, Ohno S, Ohno Y, Takakura M, Kyo S, Soma G, Sugiyama H, Inoue M (2011) WT1 peptide vaccine stabilized intractable ovarian cancer patient for one year: a case report. Anticancer Res 31:2441–2445

Eisenhauer EA, Therasse P, Bogaerts J, Schwartz LH, Sargent D, Ford R, Dancey J, Arbuck S, Gwyther S, Mooney M, Rubinstein L, Shankar L, Dodd L, Kaplan R, Lacombe D, Verweij J (2009) New response evaluation criteria in solid tumours: revised RECIST guideline (version 1.1). Eur J Cancer 45:228–247

Harries M, Gore M (2002) Part II chemotherapy for epithelial ovarian cancer-treatment of recurrent disease. Lancet Oncol 3:537–545

Hashii Y, Sato E, Ohta H, Oka Y, Sugiyama H, Ozono K (2010) WT1 peptide immunotherapy for cancer in children and young adults. Pediatr Blood Cancer 55:352–355

Izumoto S, Tsuboi A, Oka Y, Suzuki T, Hashiba T, Kagawa N, Hashimoto N, Maruno M, Elisseeva OA, Shirakata T, Kawakami M, Oji Y, Nishida S, Ohno S, Kawase I, Hatazawa J, Nakatsuka S, Aozasa K, Morita S, Sakamoto J, Sugiyama H, Yoshimine T (2008) Phase II clinical trial of Wilms tumor 1 peptide vaccination for patients with recurrent glioblastoma multiforme. J Neurosurg 108:963–971

Koensgen D, Stengel D, Belau A, Klare P, Oskay-Oezcelik G, Steck T, Camara O, Mustea A, Sommer H, Coumbos A, Bogenrieder T, Lichtenegger W (2008) North-Eastern german society of gynecological oncology study group-ovarian cancer. Topotecan and carboplatin in patients with platinum-sensitive recurrent ovarian cancer. Results of a multicenter NOGGO: phase I/II study. Cancer Chemother Pharmacol 62:393–400

Markman M, Webster K, Zanotti K, Kulp B, Peterson G, Belinson J (2003) Phase 2 trial of single-agent gemcitabine in platinum-paclitaxel refractory ovarian cancer. Gynecol Oncol 90:593–596

Morita S, Oka Y, Tsuboi A, Kawakami M, Maruno M, Izumoto S, Osaki T, Taguchi T, Ueda T, Myoui A, Nishida S, Shirakata T, Ohno S, Oji Y, Aozasa K, Hatazawa J, Udaka K, Yoshikawa H, Yoshimine T, Noguchi S, Kawase I, Nakatsuka S, Sugiyama H, Sakamoto J (2006) A phase I/II trial of a WT1 (Wilms' tumor gene) peptide vaccine in patients with solid malignancy: safety assessment based on the phase I data. Jpn J Clin Oncol 36:231–236

Nishio S, Katsumata N, Matsumoto K, Tanabe H, Kato Y, Yonemori K, Kouno T, Shimizu C, Ando M, Fujiwara Y. (2006) Analysis of third-line and forth-line chemotherapy for recurrent ovarian cancer treated with first-line platinum/taxane regimens 2006 ASCO Annual Meeting Proceedings Part I. J Clin Oncol 24 (18S June 20 Supplement):15045

Ohno S, Kyo S, Myojo S, Dohi S, Ishizaki J, Miyamoto K, Morita S, Sakamoto J, Enomoto T, Kimura T, Oka Y, Tsuboi A, Sugiyama H, Inoue M (2009) Wilms' tumor 1 (WT1) peptide immunotherapy for gynecological malignancy. Anticancer Res 29:4779–4784

Oji Y, Oka Y, Nishida S, Tsuboi A, Kawakami M, Shirakata T, Takahashi K, Murao A, Nakajima H, Narita M, Takahashi M, Morita S, Sakamoto J, Tanaka T, Kawase I, Hosen N, Sugiyama H (2010) WT1 peptide vaccine induces reduction in minimal residual disease in an imatinib-treated CML patient. Eur J Haematol 85:358–360

Oka Y, Sugiyama H (2010) WT1 peptide vaccine, one of the most promising cancer vaccines: its present status and the future prospects. Immunotherapy 2:591–594

Vergote I, Finkler N, del Campo J, Lohr A, Hunter J, Matei D, Kavanagh J, Vermorken JB, Meng L, Jones M, Brown G, ASSIST-1 Study Group (2009) Phase 3 randomised study of canfosfamide (Telcyta, TLK286) versus pegylated liposomal doxorubicin or topotecan as third-line therapy in patients with platinum-refractory or resistant ovarian cancer. Eur J Cancer 45:2324–2332

Cytokine gene expression signature in ovarian clear cell carcinoma

NOZOMU YANAIHARA[1], MICHAEL S. ANGLESIO[2], KAZUNORI OCHIAI[1], YUKIHIRO HIRATA[1], MISATO SAITO[1], CHIE NAGATA[1], YASUSHI IIDA[1], SATOSHI TAKAKURA[1], KYOSUKE YAMADA[1], TADAO TANAKA[1] and AIKOU OKAMOTO[1]

[1]Department of Obstetrics and Gynecology, The Jikei University School of Medicine, Tokyo, Japan; [2]Department of Pathology, University of British Columbia, Vancouver, British Columbia, Canada

Received March 16, 2012; Accepted May 18, 2012

DOI: 10.3892/ijo.2012.1533

Abstract. Cytokine expression in a tumor microenvironment can impact both host defense against the tumor and tumor cell survival. In this study, we sought to clarify whether the cytokine gene expression profile could have clinical associations with ovarian cancer. We analyzed the expression of 16 cytokine genes (*IL-1α, IL-1β, IL-2, IL-4, IL-5, IL-8, IL-10, IL-12p35, IL-12p40, IL-15, IFN-γ, TNF-α, IL-6, HLA-DRA, HLA-DPA1* and *CSF1*) in 50 ovarian carcinomas. Hierarchical clustering analysis of these tumors was carried out using Cluster software and differentially expressed genes were examined between clear cell carcinoma (CCC) and other subtypes. Following this examination we evaluated the biological significance of *IL-6* knockdown in CCC. Unsupervised hierarchical clustering analysis of cytokine gene expression revealed two distinct clusters. The relationship between the two clusters and clinical parameters showed statistically significant differences in CCC compared to other histologies. CCC showed a dominant Th-2 cytokine expression pattern driven largely by *IL-6* expression. Inhibition of IL-6 in CCC cells suppressed Stat3 signaling and rendered cells sensitive to cytotoxic agents. The unique cytokine expression pattern found in CCC may be involved in the pathogenesis of this subtype. In particular, high *IL-6* expression appears likely to be driven by the tumor cells, fueling an autocrine pathway involving IL-6 expression and Stat3 activation and may influence survival when exposed to cytotoxic chemotherapy. Modulation of IL-6 expression or its related signaling pathway may be a promising strategy of treatment for CCC.

Introduction

Ovarian cancer is the most lethal gynecological malignancy worldwide; in Japan alone it is estimated that there were 7913 new cases of ovarian cancer and 4415 cases of mortality due to this disease in 2006 (Center for Cancer Control and Information Services, National Cancer Center, Japan). Overall, ovarian cancer patients respond to cytoreductive surgery and platinum and taxane based combination chemotherapy, however, advanced cases have a high recurrence rate and the 5-year survival rate has remained largely unchanged since the 1980s, being close to 30% (1). This, however, is skewed, given the mass of recent evidence suggesting that histological subtypes of ovarian cancer represent unique diseases, that the majority of cases (50-70%) are of serous histology, and that all ovarian carcinoma subtypes are still treated with a 'one size fits all' approach. Serous cancers seem to initially respond well to platinum and taxane chemotherapy, whereas other subtypes respond poorly or not at all (2-5). These data are finally initiating separate clinical trials for unique subtypes such as clear cell carcinoma (CCC) (6) and mucinous adenocarcinoma (MA) (7). Even within histologically defined groups, such as high-grade serous tumors, molecular subtypes are emerging. Defining molecular mechanisms involved in the development and progression of ovarian cancer and their interaction with host defenses is integral to the development of novel therapeutic approaches and successful treatment stratification.

Factors intrinsic to the tumor and the host influence progression, host defense against tumors is controlled by several immunological mediators that play an important role in the host-tumor immune system conflict (8). The host-tumor immune response is in part regulated by CD4 helper T-lymphocytes, Th1 and Th2 cells. Th1 cells produce proinflammatory cytokines and drive the cell-mediated immune response, while Th2 cells regulate humoral immunity by expressing anti-inflammatory cytokines. Alterations of cytokine expression and an imbalance in Th1/Th2 cytokine response have previously been observed in ovarian carcinomas (9-11). Serous adenocarcinoma (SA) is frequently subject to infiltration by activated T cells (TILs; tumor infiltrating lymphocytes), and patients with dense infiltrates of $CD3^+$ $CD8^+$ T cells had a more favorable prognosis while infiltration of other cell types, including $CD4^+$ $CD25^+$ $FoxP3^+$ regulatory T cells, opposed antitumor immunity (9).

Seike *et al* reported that a unique cytokine gene expression signature of noncancerous lung tissue and corresponding tumor tissue in lung adenocarcinoma predicted metastasis and disease progression (12). The prognostic signature consisted mainly of cytokine genes that were expressed in Th1 and Th2

Correspondence to: Dr Nozomu Yanaihara, Department of Obstetrics and Gynecology, The Jikei University School of Medicine 3-25-8 Nishi-Shinbashi, Minato-ku, Tokyo 105-8461, Japan
E-mail: yanazou@jikei.ac.jp

Key words: cytokine, expression signature, IL-6, clear cell carcinoma, stat3

cells. Taken together, these findings suggest that alterations in cytokine gene expression of tumors could be involved in the pathogenesis of other types of cancer, including ovarian cancer.

In this study, we sought to clarify whether the cytokine gene expression profile could have clinical associations with ovarian cancer by focusing on the expression profile of 12 cytokine genes in 50 ovarian cancers. We found that a cytokine gene expression signature of ovarian cancer could distinguish the histological subtype, and a unique expression pattern found in CCC may be involved in the pathogenesis of this ovarian cancer subtype. We further evaluated the biological significance of *IL-6* overexpression in CCC using siRNA and found that the drug resistance phenotype in CCC might be regulated by the activated IL-6 signaling pathway including Stat3 activation.

Materials and methods

Clinical samples and cell lines. Tumor specimens were surgically obtained from patients with primary ovarian carcinoma who were treated at the Department of Obstetrics and Gynecology, The Jikei University School of Medicine. The Jikei University School of Medicine Ethics Review Committee approved the study protocol and informed consent was obtained from all patients. Tumors were staged in accordance with the International Federation of Gynecology and Obstetrics (FIGO) system (1988). Fifty tumor RNA specimens that passed quality control standards were used to identify a gene signature. Clinical and pathological characteristics of the 50 patients are shown in Table I. Forty-seven patients received first-line platinum-based chemotherapy.

Seven human CCC cell lines (JHOC-5, JHOC-7, JHOC-8, JHOC-9, HAC-2, RMG-I, and RMG-II) and five human ovarian non-CCC cell lines were used in this study. JHOC-5, JHOC-7, JHOC-8, and JHOC-9 were obtained from Riken BioResource center (Tsukuba, Japan). HAC-2 was kindly provided by Dr M. Nishida (Tsukuba University, Tsukuba, Japan). RMG-I and RMG-II were kindly provided by Dr D. Aoki (Keio University, Tokyo, Japan). A2780 (undifferentiated carcinoma) was provided by Dr E. Reed (NCI, Bethesda, MD) and 2008 (SA) was provided by Dr S.B. Howell (UCSD; San Diego, CA). SKOV3 (SA), MCAS (MA), and Tyk-nu (undifferentiated carcinoma) were obtained from ATCC (Rockville, MD). RMG-I and RMG-II were maintained in Ham's F12 medium (Sigma-Aldrich, Tokyo, Japan) with 10% fetal bovine serum (FBS), and the other cells were cultured in RPMI-1640 (Sigma-Aldrich) containing 10% FBS.

Quantitative reverse transcription-polymerase chain reaction analysis. All tissue was freshly collected during surgery and stored at -80˚C. Cryostat sections containing >80% cancer cells were prepared as tumor specimens. Total RNA was isolated with TRIzol reagent (Invitrogen, Carlsbad, CA). Total RNA (3 μg) was converted to complementary DNA (cDNA) with random hexamers and SuperScript III First-Strand Synthesis kit (Invitrogen). The cDNAs were then used for qRT-PCR analysis of 16-gene expression profile. Normal ovarian tissue from a patient who had undergone surgical resection was used as a reference for each tissue sample.

Table I. Clinical and pathological characteristics of the 50 ovarian cancer patients.

Parameters	No. of patients	% of patients
Patient age		
≤60 years	41	82
>60 years	9	18
FIGO stage		
I	19	38
II	3	6
III	22	44
IV	6	12
Histological type		
SA	24	48
EA	5	10
CCC	21	42
Residual tumor		
≤1 cm	32	64
>1 cm	18	36

SA, serous adenocarcinoma; EA, endometrioid adenocarcinoma; CCC, clear cell carcinoma.

Several studies have suggested that normal ovarian tissue and even surface ovarian epithelium may not be the tissue of origin for many ovarian epithelial malignancies (13), therefore the use of ovarian tissue as a reference for qRT-PCR is arbitrary and not meant for a direct comparison of subtypes to normal ovarian tissue but rather for an intercomparison of tumor samples. The expression profiles of 12 cytokine genes [i.e., interleukin 1α (*IL-1α*), interleukin 1β (*IL-1β*), interleukin 2 (*IL-2*), interleukin 4 (*IL-4*), interleukin 5 (*IL-5*), interleukin 8 (*IL-8*), interleukin 10 (*IL-10*), interleukin 12 p35 (*IL-12p35*), interleukin 12 p40 (*IL-12p40*), interleukin 15 (*IL-15*), interferon γ (*IFN-γ*) and tumor necrosis factor-α (*TNF-α*)] were quantified with the use of TaqMan Cytokine Gene Expression Plates (Applied Biosystems, Foster City, CA). Additional individual Taqman assays (Applied Biosystems) were also used to measure expression of interleukin 6 (*IL-6*), major histocompatibility complex (MHC) class II antigen DR α (*HLA-DRA*), MHC class II antigen DP α 1 (*HLA-DPA1*), and colony stimulating factor 1 (*CSF1*). All PCR reactions were performed with a StepOnePlus Real-Time PCR System (Applied Biosystems), Human 18S ribosomal RNA (rRNA) labeled with VIC reporter dye (Applied Biosystems) was used as an endogenous control. Gene expression was quantified using the comparative method ($2^{-\Delta\Delta CT}$), where C_T = threshold cycle, $\Delta\Delta C_T = (C_T$ cytokine - C_T 18S rRNA) - (C_T reference - C_T 18S rRNA), as previously described (14). To ensure RNA of sufficient quality and eliminate spurious amplification artifacts, all samples were required to have average CT values for cytokine genes >35 cycles, as previously described (12).

Small interfering RNA and cytotoxicity assays. Small interfering RNA (siRNA) transfection was performed using Lipofectamine™ RNAiMAX (Invitrogen). Briefly, HAC-2 and

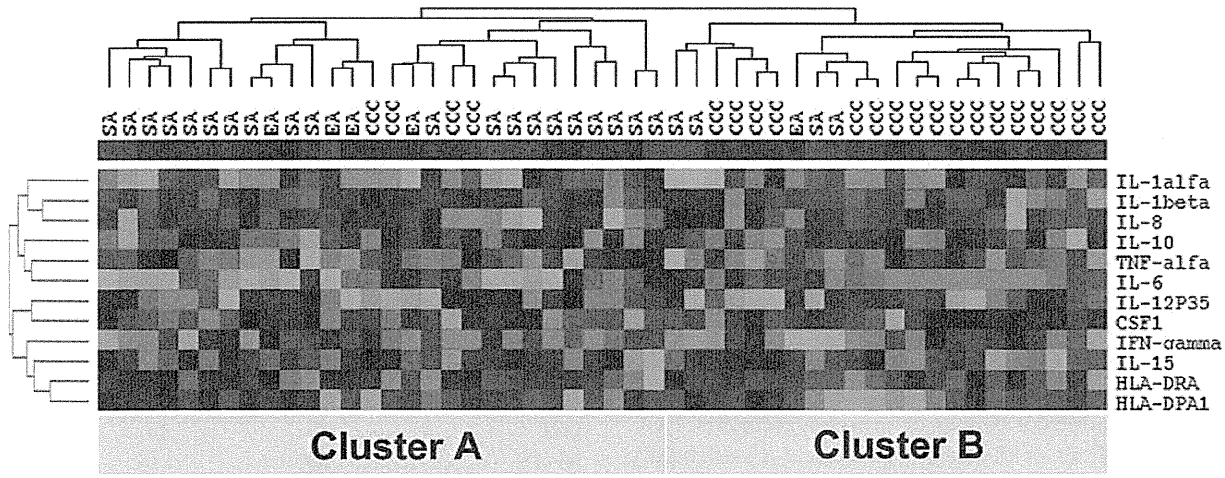

Figure 1. Expression profile of 12 cytokine genes in 50 ovarian cancer samples. Tissue samples and genes were analyzed for the calculated centered correlation distance and average linkage according to the ratios of their abundance to the median abundance of all genes among all samples. Unsupervised hierarchical clustering from these cases showed the two main trees with their corresponding histological types, i.e. cluster A and cluster B.

JHOC-5 cells were seeded at $1.5x10^5$ in a 6 cm dish, validated Stealth RNAi™ siRNA for IL-6 (Invitrogen), or stealth RNAi siRNA negative control (Invitrogen), were transfected at a final concentration of 2.5 nM. After 24 h of transfection, cells were re-seeded in 96-well plates with various concentrations of cisplatin or paclitaxel. *In vitro* cytotoxicity was measured after 96 h by means of the MTS assay using CellTiter 96 AQueous One Solution (Promega, Madison, WI). MTS solution was added to each well and incubated for 4 h. Absorbance was measured at 490 nm using a microplate reader. Data were collected as the average absorbance of three wells in any one experiment and is presented from three independent experiments; mean ± 1 standard deviation.

Western blot analysis. Total cell lysates were prepared in 1X RIPA lysis buffer and protein concentration was determined by the DC Protein Assay (Bio-Rad, Hercules, CA). Total protein (40 μg) was resolved on gradient NuPage 4-12% Bis-Tris gels (Invitrogen) and immunoblotted with specific antibodies: anti-Stat3 (clone 79D7; 1:2000), pStat3 (clone D3A7; 1:500), and β-actin (clone 13E5; 1:1000) from Cell Signaling Technology (Beverly, MA); anti-IL-6Rα (clone C-20; 1:1000) from Santa Cruz Biotechnology (Santa Cruz, CA). All blots were incubated with primary antibodies diluted in TBS with 0.1% Tween-20 and 5% bovine serum albumin overnight at 4 °C with gentle agitation. Horseradish peroxidase (HRP)-conjugated secondary antibody (Cell Signaling Technology; 1:10000) was diluted in TBS with 0.1% Tween-20 and 5% nonfat milk for 1 h at room temperature with gentle agitation. Positive immunoreactions were detected using ImmunoStar LD chemiluminescence system (Wako, Tokyo, Japan).

Statistical analysis. Unsupervised hierarchical clustering analysis was performed with Gene Cluster 3.0 (http://genexpress.stanford.edu/tutorials/cluster_view.html; Stanford University, Palo Alto, CA) and visualized with Tree View (http://genexpress.stanford.edu/tutorials/tree_view.html; Stanford University). Tissue samples and genes were analyzed for the calculated centered correlation distance and average linkage according to the ratios of their abundance to the median abundance of all genes among all samples as previously described (12). The correlation between sample clusters and clinical parameters was analyzed using the Fisher's exact test, with $p<0.05$ considered to indicate statistically significant differences.

In class comparison analysis using BRB-ArrayTools, we identified genes that were differently expressed among groups using t-test with univariate permutation tests to evaluate the significance of individual genes and correct for multiple hypothesis testing. The proportion of the permutations of the class label giving a t-test p-value as small as obtained with the true class labels is the univariate permutation p-value for that gene. The false discovery rate (FDR) associated with a row of the table is an estimate of the proportion of the genes with univariate p-values less than or equal to the one in that row that represent false positives.

A 2-sided Student's t-test was used to evaluate the sensitivity of cytotoxic agents in ovarian cancer cell lines with $p<0.05$ considered to indicate statistically significant differences.

Results

Hierarchical clustering analysis of ovarian cancer. To investigate the role of cytokine gene expression in ovarian cancer, we first analyzed the expression of 16 cytokine genes in tumor specimens from 50 primary ovarian cancers. These 16 genes were previously shown to be part of a unique inflammation/immune response-related signature in lung adenocarcinoma patients (12). Expression of *IL-2*, *IL-4*, *IL-5*, and *IL-12p40* genes was below the detectable threshold across our sample set and were therefore not carried forward in subsequent analysis. Unsupervised hierarchical clustering analysis of the 50 ovarian cancer samples, which was based on the similarities in expression patterns of the remaining 12-gene panel, revealed two distinct main clusters, namely cluster A (n=28) and cluster B (n=22) (Fig. 1). Examination of the relationship between the two clusters and clinicopathological features revealed statisti-

cally significant differences between cluster A and cluster B with respect to histological type (Table II). Cluster A consisted of 20 SA cases (83%), 4 EA cases (80%) and 4 CCC cases (19%), and the cluster B included 4 cases of SA (17%), one EA case (20%) and 17 cases of CCC (81%). In addition, there was a marginally significant difference between the two clusters and FIGO stage. However, there was no statistically significant difference in age, residual tumor size, and patient prognosis between the clusters (data not shown). Of particular note, cases in cluster B showed higher expression of Th2-related cytokine genes including *IL-6*, *IL-8*, and *IL-10*.

Given a trend for CCC and non-CCC across the two clusters we further examined the normalized expression data comparing histological classes of ovarian carcinoma, CCC vs. non-CCC. Four of the twelve genes had a statistically significant difference in expression between groups at $p<0.05$ with univariate permutation test (Table III). Among them, the expression level of *IL-6* was the most significant gene in CCC compared to non-CCC.

IL-6 expression and IL-6 siRNA transfection in ovarian cancer cell lines. Next, we analyzed the *IL-6* gene expression in twelve ovarian cancer cell lines including seven CCC cell lines. Consistent with the data obtained from surgical samples, the *IL-6* gene expression of CCC cell lines was typically higher than that of non-CCC cell lines (Fig. 2A). To begin to address whether the endogenous production of IL-6 by CCC could have biological significance of CCC, we inhibited expression of *IL-6* in CCC cells using the siRNA approach and examined the effects of *IL-6* expression on the cell growth and drug sensitivity. Expression of the *IL-6* gene was significantly decreased 24 h after *IL-6* siRNA transfection in HAC-2 and JHOC-5 (Fig. 2B). The biological effect on cell proliferation was analyzed by cell count after transfection of *IL-6* siRNA in CCC cell lines. No significant effect on cell proliferation was observed when compared to transfection of negative control siRNA (data not shown).

Although there was no change in proliferation, IL-6 inhibition did modulate downstream signaling. Stat3 is a major signaling effector of IL-6 and has been shown to be required for survival in multiple cancer models (15). Suppression of IL-6 reduced activation of Stat3 (pStat3) without affecting overall levels of Stat3 or other components of the signaling pathway (IL-6Rα; Fig. 3A). Given these effects on a pro-survival pathway we next evaluated the susceptibility of CCC cell lines to cytotoxic agents after suppression of *IL-6*. *IL-6* siRNA transfected HAC-2 exhibited a statistically significant increase in cell death to both paclitaxal (IC_{50} was 4.78±0.21 μM) and cisplatin (IC_{50} was 1.14±0.02 μM) as compared with negative control siRNA transfected cells (IC_{50} for paclitaxal was 9.82±0.41 μM and for cisplatin 2.12±0.01 μM, respectively) (Fig. 3B). Similar results were obtained from JHOC-5 cells. These results indicate that inhibition of endogenous IL-6 in CCC cells decreases Stat3 activation and sensitizes these cells to cytotoxic stress.

Table II. Clinicopathological characteristics of the 50 ovarian cancer samples by unsupervised hierarchical cluster group.

Parameters	Cluster A (n=28)	Cluster B (n=22)	p-value
Patient age			
≤60 years	23	18	0.733
>60 years	5	4	
Histological type			
SA+EA	24	5	<0.001
CCC	4	17	
FIGO stage			
I+II	9	13	0.105
III+IV	19	9	
Residual tumor			
≤1 cm	17	16	0.373
>1 cm	11	6	

SA, serous adenocarcinoma; EA, endometrioid adenocarcinoma; CCC, clear cell carcinoma.

Table III. Cytokine genes differentially expressed among CCC vs. non-CCC.

Gene	p-value	FDR	Permutation p-value
IL-6	<1e-07	<1e-07	<1e-07
IL-12p35	0.0255652	0.105	0.0237
IL-1β	0.0262116	0.105	0.0249
IL-10	0.0384981	0.115	0.0375

The four genes are significant at 0.05 level of the univariate test. Permutation p-values for significant genes were computed based on 10000 random permutations.

Discussion

Cytokine expression within a tumor microenvironment plays a fundamental role in cancer development and progression; tumor cells that produce immunosuppressive cytokines can escape the host immune response. In ovarian cancer, several cytokines associated with cellular immunity were correlated to cancer development and patient prognosis, including TNF-α, IFN-γ, IL-6, and MHC molecules (9). We report here that the expression profile of 12 pro- and anti-inflammatory cytokine genes in tumor could reliably distinguish the CCC histopathological classification of ovarian carcinoma from other epithelial subtypes. Overall evidence suggested CCC to have a Th-2 cytokine dominant expression pattern, including high levels of IL-6. In our series, 17 of 19 stage III/IV cases (89%) in cluster A were SA and 12 of 13 stage I/II cases (92%) in cluster B were CCC. It should also be noted that since >50% of CCC is diagnosed at an early stage, as seen in this study (67%), the marginal association between the expression signature and FIGO stage is likely the result of confounded representation of CCC in cluster B.

CCC differs considerably from the other histological types of ovarian cancer with respect to its clinical and molecular characteristics (5,16,19,20). With respect to cytokine expression signature and pathway activation, Yamaguchi *et al*

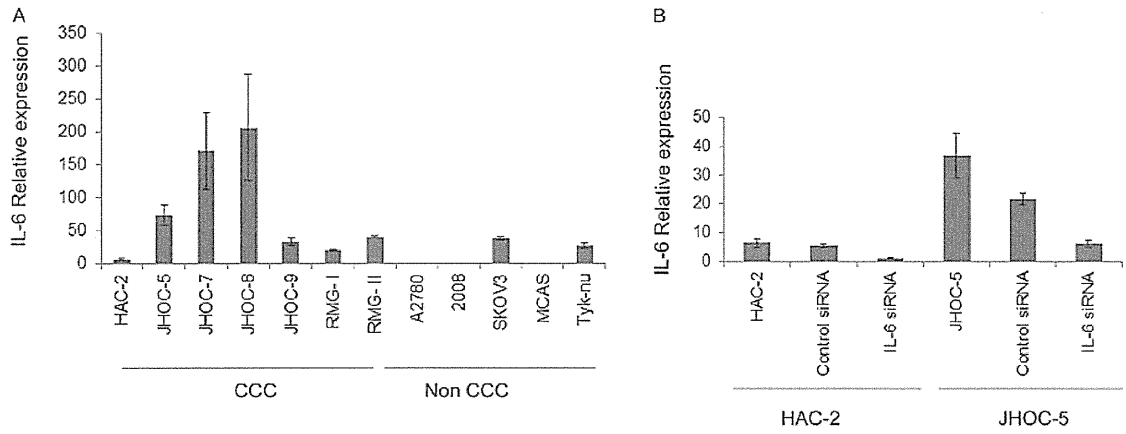

Figure 2. *IL-6* expression and *IL-6* siRNA transfection in ovarian cancer cell lines. Gene expression was quantified using the comparative method and normal ovarian tissue was used as a reference for each sample. Human 18S rRNA was used as an endogenous control. Data are shown as the mean ± SD. (A) Relative expression of the *IL-6* gene in seven CCC cell lines and five non-CCC cell lines. (B) *IL-6* and negative control siRNA transfection in CCC cell lines. Expression of the *IL-6* gene was decreased 24 h after *IL-6* siRNA transfection in HAC-2 and JHOC-5 cells.

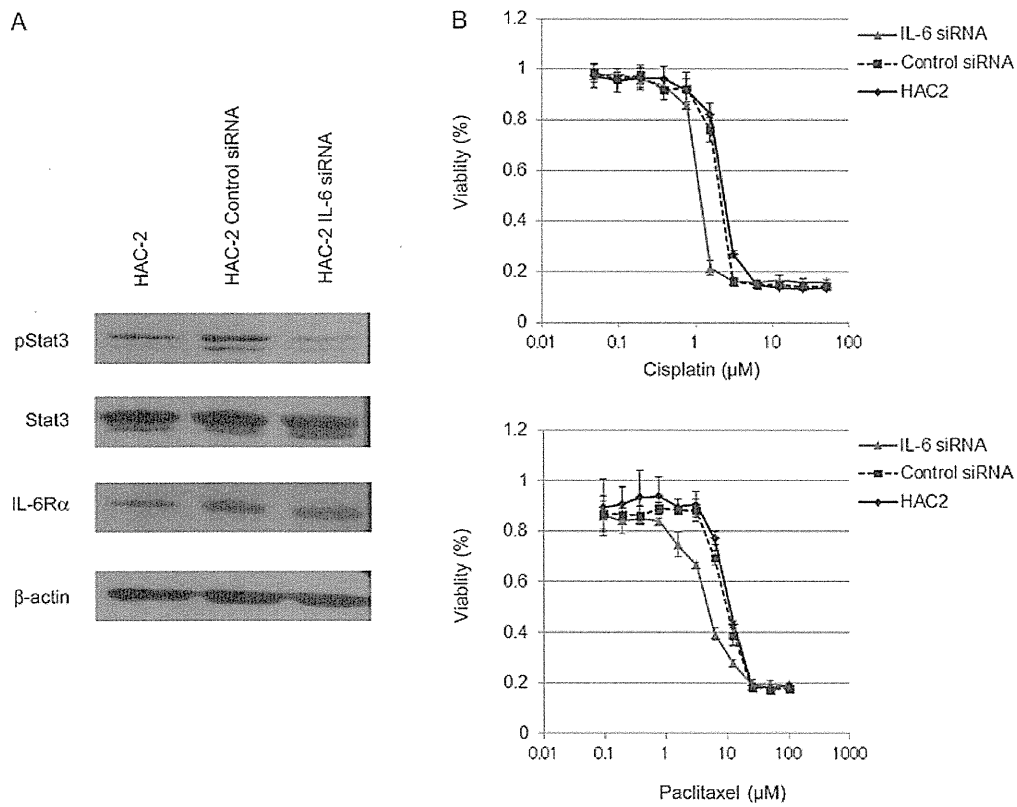

Figure 3. Effect of IL-6 expression on the responsiveness of CCC cell to paclitaxel and cisplatin. (A) Sensitivity to paclitaxel and cisplatin was measured by MTS assay in HAC-2. (B) Phosphorylated Stat3, total Stat3 and IL-6Rα expression levels were analyzed in HAC-2 cells transfected with either *IL-6* siRNA or negative control siRNA. β-actin was also used as loading control.

identified a CCC cell line specific gene signature from a large set of microarray data that contained *IL-6*, consistent with data presented here, as well as several previously known CCC markers such as *HNF-1β* (20). Our data further supports findings that implicate the activated Stat3 signaling pathway in CCC cells (19,20), with specific overexpression IL-6 in CCC compared to SA amongst the 12-cytokine panel examined and suppression of Stat3 signaling when IL-6 was knocked down with siRNA. These findings also suggest that the tumor cells, rather than the host-microenvironment, is the source of IL-6 expression. This is in contrast to previous work with high-grade SA where a subset of this histological type is associated with tumor infiltrating lymphocytes (TILs) (5,17,18). In these SA-specific studies the dominant cytokine expression pattern is presumed to be driven by the non-tumor microenvironment. However, given the modest number of samples in this study

and the overall prevalence of TILs amongst high-grade SA, it seems unlikely that TILs alone are influencing the expression pattern of cytokines in the serous tumors examined here. Markedly, expression profiling has suggested that high-grade SA with the highest levels of IL-6 are not those with TILs (18).

One of the most clinically important biological features of CCC is its inherent chemoresistance, which is associated with its poor prognosis particularly at advanced stages. Several mechanisms involved in drug resistance in CCC have been proposed, however, the precise mechanisms underlying chemoresistance remain to be elucidated (16). In this study, siRNA-mediated IL-6 expression did not directly affect proliferation, however, we found that IL-6 inhibition did reduce Stat3 activation and increase the sensitivity of CCC cell lines to both cisplatin and paclitaxel. IL-6 is a pleiotropic cytokine that plays important roles in the immune response and inflammation. Aberrant expression of *IL-6* has been implicated in many types of cancer, and the role of IL-6 in chemoresistance has been addressed in several malignancies, including multiple myeloma, renal cell carcinoma, cholangiocarcinoma, prostate cancer, and breast cancer (21). A clear link between an IL-6 rich tumor microenvironment and tumor progression or survival has been observed in other tumor models (15). Recent evidence indicates that autocrine and paracrine effects by constitutive production of IL-6 in ovarian cancer could be involved in the tumorigenic potential through the regulation of angiogenesis (22) or MMP secretion (23). These results suggest that a drug resistant phenotype in CCC may, in part, be explained by the activated autocrine IL-6 signaling pathway including Stat3 activation. It is interesting to speculate on a biological link between recently discovered endometriosis associated ovarian cancer *ARID1A* mutations (24,25), chemoresistance, and the cytokine profile specific to CCC. Though not clearly established in this context, modulation of gene expression controlled by the SWI/SNF chromatin binding complex, specifically the BRG1 component, has been shown to be required for induction of cytokine genes, including IL-6, during inflammatory responses (26).

Finally, although SA and CCC behave like distinct entities, a chemoresistant mechanism converging around the IL-6 pathway may be highly relevant to both CCC and at least some high-grade SA. Wang *et al* showed that IL-6 secreted by serous type ovarian cancer cells might contribute to the chemoresistance through the downregulation of caspase-3 and increased expression of both multidrug resistance-related genes and apoptosis inhibitory proteins (27). High IL-6 levels in the serum and ascites of ovarian cancer have been found to be associated with poor prognosis and chemoresistance (21). Most studies on this topic, however, have not differentiated between histological subtypes. More recently, blockage of IL-6 signaling by a monoclonal anti-IL-6 antibody siltuximab (CNTO 328) with cytotoxic agent has been shown to disrupt cancer progression in serous ovarian cancer cell lines both *in vitro* and in mouse xenograft models (28). Siltuximab decreased Stat3 phosphorylation and protein levels of downstream effectors including MCL-1, Bcl-XL, and Survivin in paclitaxel resistant ovarian cancer cell lines. This is consistent with decreased levels of phospho-Stat3 and chemo-sensitization observed in this report. In the phase II clinical trial with platinum-resistant ovarian cancer, siltuximab had some therapeutic activity (29). Exposure of ovarian cancer cells to siltuximab had no effect on cell growth, also consistent with our siRNA-mediate *IL-6* knockdown experiments. This has led to the hypothesis that the growth inhibitory effects of IL-6 knockdown may be evident only with tumor-stromal influences. Functional *in vivo* model systems paired with immunohistochemical and molecular analysis are needed to further refine the roles of various immune cells contributing to the molecular pathogenesis of ovarian cancer. In particular, the IL-6 related mechanism of chemo-resistance in both CCC and high-grade SA, direct inhibition of IL-6, IL-6R or other downstream signaling effectors, such as Stat3, should not be overlooked. Nonetheless, the results obtained in this study support the idea of targeting the IL-6 signaling pathway in a combination therapy approach sensitizing CCC tumor cells in particular to current gold-standard chemotherapies already in use for ovarian carcinoma.

Acknowledgements

This work was supported in part by Grants-in-Aid for Scientific Research from Japan Society for the Promotion of Science to N.Y., A.O., K.Y., and S.T., and by the Japanese Ministry of Health, Labour and Welfare to K.O. Analyses were performed using BRB ArrayTools developed by Dr Richard Simon and Amy Peng Lam.

References

1. Vaughan S, Coward JI, Bast RC Jr, *et al*: Rethinking ovarian cancer: recommendations for improving outcomes. Nat Rev Cancer 23: 719-725, 2011.
2. Köbel M, Kalloger SE, Boyd N, *et al*: Ovarian carcinoma subtypes are different diseases: implications for biomarker studies. PLoS Med 5: e232, 2008.
3. Swenerton KD, Santos JL, Gilks CB, *et al*: Histotype predicts the curative potential of radiotherapy: the example of ovarian cancers. Ann Oncol 22: 341-347, 2010.
4. Gilks CB, Ionescu DN, Kalloger SE, *et al*: Tumor cell type can be reproducibly diagnosed and is of independent prognostic significance in patients with maximally debulked ovarian carcinoma. Hum Pathol 39: 1239-1251, 2008.
5. Anglesio MS, Carey MS, Köbel M, *et al*: Clear cell carcinoma of the ovary: A report from the first Ovarian Clear Cell Symposium, June 24th, 2010 (Review). Gynecol Oncol 121: 407-415, 2010.
6. Takakura S, Takano M, Takahashi F, *et al*: Japanese Gynecologic Oncology Group. Randomized phase II trial of paclitaxel plus carboplatin therapy versus irinotecan plus cisplatin therapy as first-line chemotherapy for clear cell adenocarcinoma of the ovary: a JGOG study. Int J Gynecol Cancer 20: 240-247, 2010.
7. Shimada M, Kigawa J, Ohishi Y, *et al*: Clinicopathological characteristics of mucinous adenocarcinoma of the ovary. Gynecol Oncol 113: 331-334, 2009.
8. Schreiber RD, Old LJ and Smyth MJ: Cancer immunoediting: integrating immunity's roles in cancer suppression and promotion (Review). Science 331: 1565-1570, 2011.
9. Nelson BH: The impact of T-cell immunity on ovarian cancer outcomes (Review). Immunol Rev 222: 101-116, 2008.
10. Kusuda T, Shigemasa K, Arihiro K, *et al*: Relative expression levels of Th1 and Th2 cytokine mRNA are independent prognostic factors in patients with ovarian cancer. Oncol Rep 13: 1153-1158, 2005.
11. Marth C, Fiegl H, Zeimet AG, *et al*: Interferon-gamma expression is an independent prognostic factor in ovarian cancer. Am J Obstet Gynecol 191: 1598-1605, 2004.
12. Seike M, Yanaihara N, Bowman ED, *et al*: Use of a cytokine gene expression signature in lung adenocarcinoma and the surrounding tissue as a prognostic classifier. J Natl Cancer Inst 99: 1257-1269, 2007.

13. Kurman RJ and Shih IeM: Molecular pathogenesis and extraovarian origin of epithelial ovarian cancer - shifting the paradigm. Hum Pathol 42: 918-931, 2001.
14. Bustin SA: Absolute quantification of mRNA using real-time reverse transcription polymerase chain reaction assays. J Mol Endocrinol 25: 169-193, 2000.
15. Li N, Grivennikov SI and Karin M: The unholy trinity: inflammation, cytokines, and STAT3 shape the cancer microenvironment. Cancer Cell 12: 429-431, 2011.
16. Itamochi H, Kigawa J and Terakawa N: Mechanisms of chemoresistance and poor prognosis in ovarian clear cell carcinoma (Review). Cancer Sci 99: 653-658, 2008.
17. Tsiatas ML, Gyftaki R, Liacos C, *et al*: Study of T lymphocytes infiltrating peritoneal metastases in advanced ovarian cancer: associations with vascular endothelial growth factor levels and prognosis in patients receiving platinum-based chemotherapy. Int J Gynecol Cancer 19: 1329-1334, 2009.
18. Tothill RW, Tinker AV, George J, *et al*: Novel molecular subtypes of serous and endometrioid ovarian cancer linked to clinical outcome. Clin Cancer Res 14: 5198-5208, 2008.
19. Anglesio MS, George J, Kulbe H, *et al*: IL6-STAT3-HIF signaling and therapeutic response to the angiogenesis inhibitor sunitinib in ovarian clear cell cancer. Clin Cancer Res 17: 2538-2548, 2011.
20. Yamaguchi K, Mandai M, Oura T, *et al*: Identification of an ovarian clear cell carcinoma gene signature that reflects inherent disease biology and the carcinogenic processes. Oncogene 29: 1741-1752, 2010.
21. Hong DS, Angelo LS and Kurzrock R: Interleukin-6 and its receptor in cancer: implications for translational therapeutics (Review). Cancer 110: 1911-1928, 2007.
22. Nilsson MB, Langley RR and Fidler IJ: Interleukin-6, secreted by human ovarian carcinoma cells, is a potent proangiogenic cytokine. Cancer Res 65: 10794-10800, 2005.
23. Rabinovich A, Medina L, Piura B, Segal S and Huleihel M: Regulation of ovarian carcinoma SKOV-3 cell proliferation and secretion of MMPs by autocrine IL-6. Anticancer Res 27: 267-272, 2007.
24. Jones S, Wang TL, Shih IeM, *et al*: Frequent mutations of chromatin remodeling gene ARID1A in ovarian clear cell carcinoma. Science 330: 228-231, 2010.
25. Wiegand KC, Shah SP, Al-Agha OM, *et al*: ARID1A mutations in endometriosis-associated ovarian carcinomas. N Engl J Med 363: 1532-1543, 2010.
26. Cullen SJ, Ponnappan S and Ponnappan U: Catalytic activity of the proteasome fine-tunes Brg1-mediated chromatin remodeling to regulate the expression of inflammatory genes. Mol Immunol 47: 600-605, 2009.
27. Wang Y, Niu XL, Qu Y, *et al*: Autocrine production of interleukin-6 confers cisplatin and paclitaxel resistance in ovarian cancer cells. Cancer Lett 295: 110-123, 2010.
28. Guo Y, Nemeth J, O'Brien C, *et al*: Effects of siltuximab on the IL-6-induced signaling pathway in ovarian cancer. Clin Cancer Res 16: 5759-5769, 2010.
29. Coward J, Kulbe H, Chakravarty P, *et al*: Interleukin-6 as a therapeutic target in human ovarian cancer. Clin Cancer Res 17: 6083-6096, 2011.

SCIENTIFIC REPORTS

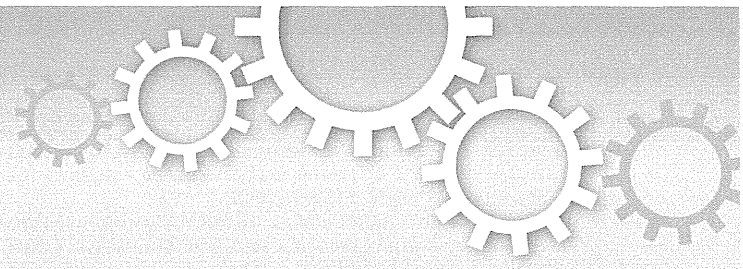

ASBEL, an ANA/BTG3 antisense transcript required for tumorigenicity of ovarian carcinoma

Satoshi Yanagida[1,2*], Kenzui Taniue[1*], Hironobu Sugimasa[1], Emiko Nasu[1], Yasuko Takeda[1], Mana Kobayashi[1], Tadashi Yamamoto[3], Aikou Okamoto[2] & Tetsu Akiyama[1]

[1]Laboratory of Molecular and Genetic Information, Institute of Molecular and Cellular Biosciences, The University of Tokyo, 1-1-1, Yayoi, Bunkyo-ku, Tokyo, 113-0032, Japan, [2]Department of Obstetrics and Gynecology, The Jikei University school of Medicine, 3-25-8, Nishi-shinbashi, Minato-ku, Tokyo, 105-8461, Japan, [3]Division of Oncology, Department of Cancer Biology, Institute of Medical Science, The University of Tokyo, 461 Shirokanedai, Tokyo, 108-8639, Japan.

SUBJECT AREAS:
OVARIAN CANCER
APOPTOSIS
LONG NON-CODING RNAS
RNA TRANSPORT

Received
22 October 2012

Accepted
22 January 2013

Published
19 February 2013

Correspondence and requests for materials should be addressed to T.A. (akiyama@iam.u-tokyo.ac.jp)

* These authors contributed equally to this work.

Mammalian genomes encode numerous antisense non-coding RNAs, which are assumed to be involved in the regulation of the sense gene expression. However, the mechanisms of their action and involvement in the development of diseases have not been well elucidated. The ANA/BTG3 protein is an antiproliferative protein whose expression is downregulated in prostate and lung cancers. Here we show that an antisense transcript of the *ANA/BTG3* gene, termed *ASBEL*, negatively regulates the levels of ANA/BTG3 protein, but not of *ANA/BTG3* mRNA and is required for proliferation and tumorigenicity of ovarian clear cell carcinoma. We further show that knockdown of ANA/BTG3 rescues growth inhibition caused by *ASBEL* knockdown. Moreover, we demonstrate that *ASBEL* forms duplexes with *ANA/BTG3* mRNA in the nucleus and suppresses its cytoplasmic transportation. Our findings illustrate a novel function for an antisense transcript that critically promotes tumorigenesis by suppressing translation of the sense gene by inhibiting its cytoplasmic transportation.

Recent studies have revealed that most mammalian genes express antisense transcripts[1,2]. The majority of antisense transcripts are non-coding RNAs (ncRNAs) complementary to a region of the sense mRNA. Sense-antisense transcript pairs so far reported include genes involved in various biological processes, development and diseases, suggesting critical roles of antisense transcripts in mammalian gene expression. In contrast to microRNAs, antisense transcripts have been suggested to exert their function through a variety of mechanisms. For example, duplex formation between sense and antisense RNAs in the nucleus can modulate mRNA alternative splicing, editing and transport[3–5]. Sense-antisense duplex formation in the cytoplasm can change sense mRNA stability and translation efficiency[6–10]. It has also been suggested that some antisense transcripts bind to the corresponding DNA strand and recruit DNA methyltransferases or histone-modifying enzymes, thereby modulating sense gene expression[11–13]. However, the exact mechanisms underlying these functions remain to be further elucidated.

ANA/BTG3 is a member of the TOB/BTG family of antiproliferative genes that regulates cell cycle progression in a variety of cell types[14]. It has also been reported that loss of ANA/BTG3 in normal cells induces cellular senescence via the ERK-JMJD3-p16(INK4a) signaling axis[15]. ANA/BTG3 expression is also known to be induced by DNA damage in a p53-dependent manner and directly represses E2F1-mediated transactivation[16]. In addition, ANA/BTG3 interacts with the CCR4 transcription factor-associated protein Caf1[17], suggesting its involvement in cytoplasmic mRNA deadenylation and turnover. Furthermore, ANA/BTG3 expression is downregulated in prostate cancer through promoter hypermethylation[18]. ANA/BTG3 expression is also reduced in the majority of lung adenocarcinoma[19]. Thus, increasing evidence suggests that ANA/BTG3 functions as a tumor suppressor.

It has been reported that the tumor suppressor functions of p53 and WT1 are regulated by their antisense transcripts[20,21]. We therefore searched for antisense transcripts encoded in other tumor suppressor genes. We found that ANA/BTG3 encodes an antisense transcript although most of the important tumor suppressor genes, including RB, APC, BRCA1, BRCA2, NF1 and NF2, do not. Here we show that an antisense transcript of *ANA/BTG3* termed *ASBEL* is required for the regulation of ANA/BTG3 protein expression and tumorigenicity of ovarian cancer.

Results

***ASBEL*, an antisense transcript of *ANA/BTG3*.** Examination of the GenBank database revealed that a highly conserved gene is encoded by the DNA strand opposite the *ANA/BTG3* gene (Fig. 1a). This gene encodes a conserved ~2-kb ncRNA (termed *ASBEL* [antisense ncRNA in the *ANA/BTG3 (three)* locus]), the 5′ region of which is complementary to a portion of the 5′untranslated region (UTR) and the first exon of *ANA/BTG3* mRNA. Strand-specific RT-PCR analysis confirmed that *ASBEL* was indeed transcribed from the DNA strand opposite to the *ANA/BTG3* gene (Fig. 1a). Northern blotting analyses showed that *ASBEL* was detected (Fig. 1b). Subcellular fractionation and RT-PCR analysis revealed that *ASBEL* was present in the nucleus (Fig. 1c and Supplementary Fig. S1), consistent with the fact that *ASBEL* is a ncRNA.

***ASBEL* is required for the tumorigenicity of ovarian cancer.** We examined *ASBEL* expression in human ovarian cancerous tissues and adjacent non-cancerous tissues (5 serous adenocarcinoma (SA), 2 endometrioid adenocarcinoma (EA), 2 clear cell adenocarcinoma (CCC), 1 mucinous adenocarcinoma (MA), 1 dysgerminoma (Dys)). The expression of *ASBEL* was higher in 8 out of 11 ovarian cancerous tissues than in the non-cancerous tissues (Fig. 2a). Thus, to clarify the importance of *ASBEL* in ovarian tumorigenesis, we knocked down *ASBEL* expression in the JHOC5 cells by infecting with a lentivirus expressing an shRNA targeting *ASBEL* (shASBEL) (Fig. 2b). MTT assays revealed that knockdown of *ASBEL* caused a significant reduction in the growth of JHOC5, JHOC9, and OVISE cells (Fig. 2c). CellTiter-Glo assays also revealed that knockdown of ASBEL using siRNA caused a significant reduction in the growth of the CCC cell lines JHOC5, JHOC9, and OVISE and the serous adenocarcinoma cell lines OV1063 and 2008 cells (Fig. 2d). Furthermore, AnnexinV assays showed that knockdown of *ASBEL* induced apoptosis of JHOC5 cells (Fig. 2e). When JHOC5 cells stably expressing shASBEL were transplanted into nude mice, cell growth was significantly retarded compared to JHOC5 cells infected with control lentivirus (Fig. 2f and Supplementary Fig. S2). Immunohistochemical analyses of tumor xenografts demonstrated that tumor cells were arranged in solid, tubular and partially papillary patterns, which represents an important feature of human ovarian cancer (Supplementary Fig. S2). These results suggest that *ASBEL* may be required for the tumorigenicity of ovarian cancer.

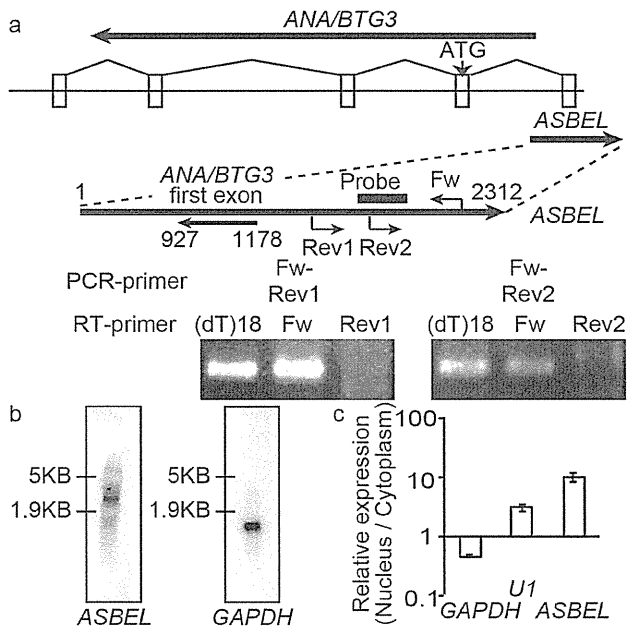

Figure 1 | *ASBEL* is transcribed from the DNA strand opposite to *ANA/BTG3*. (a) Strand-specific RT-PCR analysis of *ASBEL*. (Upper panel) Schematic representation of the genomic organization of the region containing *ASBEL* and *ANA/BTG3*. Primers for reverse transcription (RT-primer) and PCR (PCR-primer) were designed to specifically target either the sense (Fw) or antisense strand (Rev1 and Rev2) of *ASBEL*. Oligo(dT)18 was used as a positive control. "Probe" indicates the region used for Northern blot analysis. (Lower panel) RT-PCR analysis was performed using the primers indicated. Sense RT-primers generated PCR products, whereas anti-sense RT-primers did not. (b) Northern blot analysis of *ASBEL* and *GAPDH* mRNA in JHOC5 cells. (c) Subcellular localization of *ASBEL*. JHOC5 cells were subjected to subcellular fractionation and the amounts of *ASBEL* in each fraction were evaluated by RT-PCR. *GAPDH* mRNA was used as a marker specific for the cytoplasm. *U1* was used as a nuclear marker.

***ASBEL* downregulates ANA/BTG3 protein expression.** Since antisense transcripts have been reported to regulate the expression of their overlapping sense transcripts[1,2], we investigated whether knockdown of *ASBEL* could increase the expression of ANA/BTG3 in JHOC5, JHOC9 and OVISE cells. RT-PCR and immunoblotting analyses revealed that knockdown of *ASBEL* using siRNA (siASBEL) resulted in an increase in the levels of ANA/BTG3 protein, but not mRNA (Fig. 3a, b). Knockdown of ASBEL using shASBEL also did not affect the levels of ANA/BTG3 mRNA (Supplementary Fig. S3). By contrast, overexpression of *ASBEL* decreased the levels of ANA/BTG protein, but not mRNA, compared to that of *antisense ASBEL* (Fig. 3c). These results raise the possibility that the reduction in cell growth caused by *ASBEL* knockdown is due to an increase in the expression of ANA/BTG3 protein. Thus, we examined whether knockdown of ANA/BTG3 could restore the growth of cells transfected with siASBEL. We found that knockdown of ANA/BTG3 using shRNA (shANA/BTG3) could partially rescue JHOC5 cells from siASBEL-mediated growth inhibition (Fig. 3d, e). Knockdown of ANA/BTG3 did not affect *ASBEL* expression levels (Fig. 3e and Supplementary Fig. S4). Thus, *ASBEL*-mediated downregulation of ANA/BTG3 may be critical for the proliferation of ovarian cancer.

***ASBEL-ANA/BTG3* duplexes are retained in the nucleus.** To clarify the mechanisms underlying *ASBEL*-mediated downregulation of ANA/BTG3 expression, we attempted to detect *ASBEL-ANA/BTG3* RNA duplexes. We overexpressed *ASBEL* fused to an oligonucleotide coding for an RNA hairpin that binds bacteriophage pp7 coat protein (*pp7-ASBEL*) in JHOC5 cells and performed RNA immunoprecipitation (RIP) analysis. Lysates prepared from JHOC5 cells transfected with the *pp7-ASBEL*, *ANA/BTG3* mRNA and FLAG-tagged pp7 coat protein expression constructs were subjected to immunoprecipitation with anti-FLAG antibody. RT-PCR analysis revealed that *ANA/BTG3* mRNA was associated with the *pp7-ASBEL* immunoprecipitates (Fig. 4a, b). By contrast, *ANA/BTG3* mRNA was not co-precipitated when *pp7-antisense ASBEL* or *pp7*-mutant *ASBELs* (Fig. 4a, *ASBEL-Del-1* and *-4*) that lack the region complementary to *ANA/BTG3* was transfected instead of *pp7-ASBEL* (Fig. 4b, c). In addition, *pp7*-mutant *ASBELs* (Fig. 4a, *ASBEL-Del-2* and *-3*) that contain the region complementary to *ANA/BTG3* efficiently coprecipitated *ANA/BTG3* mRNA (Fig. 4c). These results suggest that *ASBEL* is able to hybridize and generate *ASBEL-ANA/BTG3* RNA duplexes.

Because only ANA/BTG3 protein, but not its mRNA levels are regulated by *ASBEL*, we speculated that *ASBEL-ANA/BTG3* RNA duplexes are retained in the nucleus. Subcellular fractionation and RT-PCR analyses showed that knockdown of *ASBEL* resulted in an increase in the amount of *ANA/BTG3* mRNA and ANA/BTG3 protein present in the cytoplasm (Fig. 4d). To directly test the possibility that *ASBEL* may influence translation, lysates from JHOC5 cells transfected with siASBEL were fractionated through sucrose

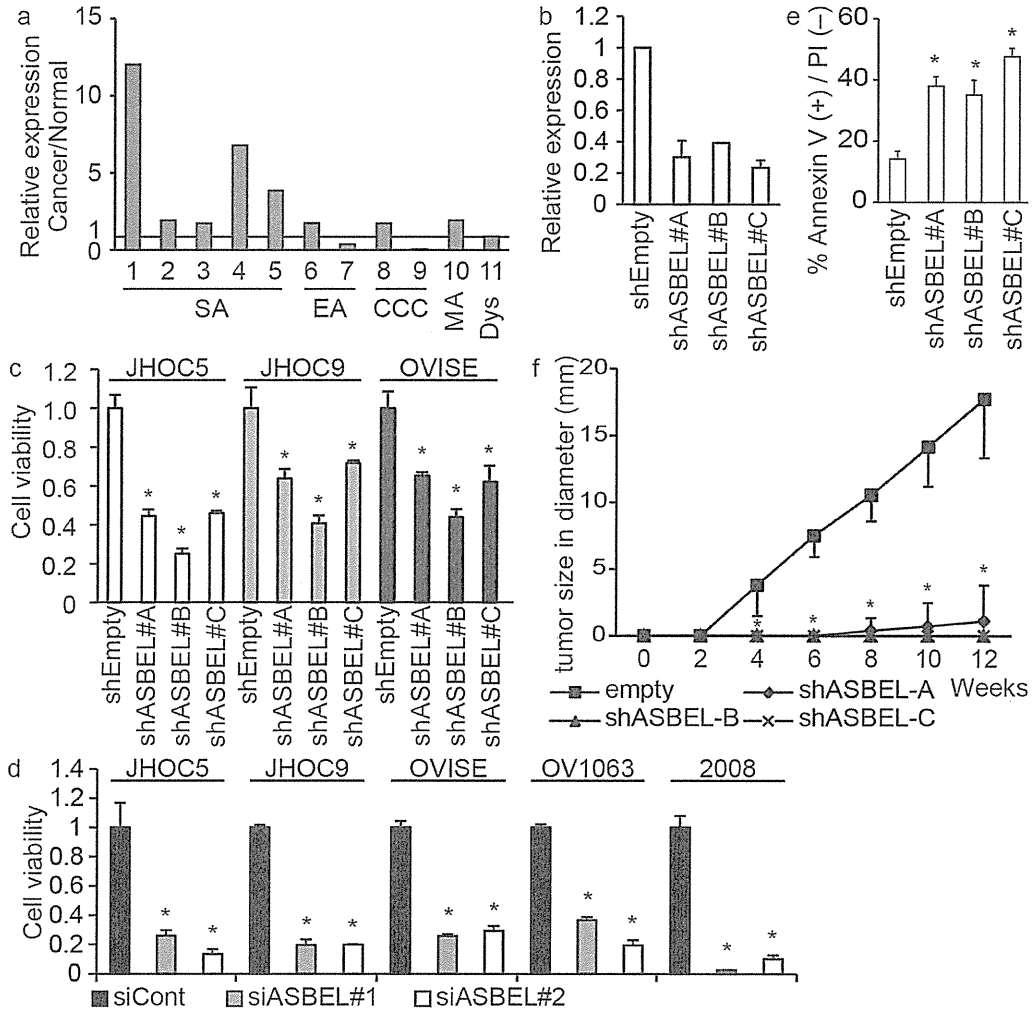

Figure 2 | Knockdown of *ASBEL* induces apoptosis of ovarian cancer cell lines. (a) qRT-PCR analysis of *ASBEL* expression in human ovarian cancerous and corresponding non-cancerous tissues. 1~5, serous adenocarcinoma; 6 and 7, endometrioid adenocarcinoma; 8 and 9, clear cell adenocarcinoma; 10, mucinous adenocarcinoma ; 11, dysgerminoma. Prior to fold-change calculation, the values were normalized to the signal generated from *GAPDH* mRNA. (b) qRT-PCR analysis of *ASBEL* expression in JHOC5 cells infected with a lentivirus harbouring an shRNA targeting *ASBEL*. Error bars represent the s.d. (n = 3). (c) Viability of ovarian cancer cell lines infected with a lentivirus expressing an shRNA targeting *ASBEL* was assessed by MTT assays. *, $P < 0.05$. (d) Viability of ovarian cancer cell lines transfected with siRNA targeting *ASBEL* was assessed by CellTiter-Glo assays. *, $P < 0.05$. (e) Annexin assays were performed with JHOC5 cells that had been infected with a lentivirus expressing an shRNA targeting *ASBEL*. *, $P < 0.05$. (f) JHOC5 cells infected with a lentivirus expressing an shRNA targeting *ASBEL* were injected into nude mice. Sizes of tumors were measured once a week using calipers. Results are expressed as the mean ± s.e.m. (1×10^5, n = 6). *, $P < 0.05$.

gradients. Knockdown of *ASBEL* did not change the polysome distribution profiles (Supplementary Fig. S5, lower panel), indicating that *ASBEL* does not affect global translation. qRT-PCR analysis of RNA isolated from each fraction revealed that knockdown of ASBEL did not induce changes in the size of polysomes translating *ANA/BTG3* and *HPRT1* mRNAs. These results suggest that *ASBEL* does not affect the translation of *ANA/BTG3* mRNA. Thus, *ASBEL* may inhibit ANA/BTG3 protein expression by forming *ASBEL-ANA/BTG3* RNA duplexes, which are retained in the nucleus (Fig. 5).

Discussion

In the present study, we have shown that *ASBEL*, a natural antisense transcript of the *ANA/BTG3* gene, negatively regulates the expression of ANA/BTG3. This is the first report showing the mechanism underlying the regulation of ANA/BTG3 expression. Furthermore, we showed that *ASBEL* is required for proliferation and tumorigenicity of ovarian cancer. Thus, we speculate that downregulation of ANA/BTG3 by *ASBEL* is critical for proliferation and tumorigenicity of ovarian cancer. This notion is supported by the results of our rescue experiments showing that knockdown of ANA/BTG3 using shRNA rescues growth inhibition caused by *ASBEL* knockdown. These results are consistent with previous reports that ANA/BTG3 plays a critical role in cell proliferation and is downregulated in prostate and lung cancers[14–16,18,19]. It is possible that *ASBEL* is also involved in the tumorigenicity of cancers other than ovarian cancer, including prostate and lung cancers. Indeed, our preliminary results show that *ASBEL* is required for proliferation and tumorigenicity of colon cancer cells.

It has been reported that antisense transcripts regulate gene expression at various steps in the post-tanscriptional processing of mRNAs[2]. We showed that *ASBEL* hybridizes and generates *ASBEL-ANA/BTG3* RNA duplexes in vivo. It is well known that mRNA expression of several genes, including *p53*, β-secretase-1 (*BACE1*) and inducible nitric oxide synthase (*INOS*), is regulated by duplex

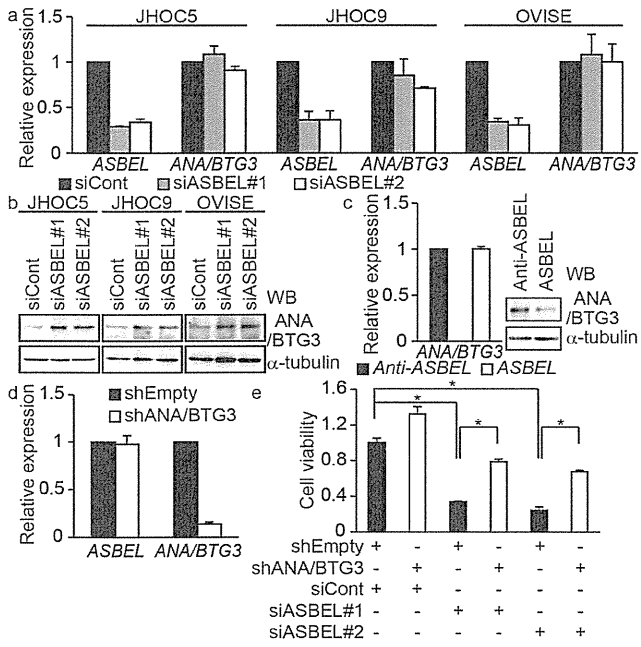

Figure 3 | *ASBEL* downregulates ANA/BTG3 protein, but not mRNA expression. (a) qRT-PCR analysis of *ASBEL* and *ANA/BTG3* expression in ovarian cancer cell lines transfected with siRNA targeting *ASBEL*. Prior to fold-change calculation, the values were normalized to the signal generated from *GAPDH* mRNA. (b) Cell lysates from ovarian cancer cell lines transfected with siRNA targeting *ASBEL* were subjected to immunoblotting analysis with antibodies against the indicated proteins. α-tubulin was used as a loading control. (c) (Left) qRT-PCR analysis of *ANA/BTG3* expression in JHOC5 cells transfected with either the *sense* or *antisense ASBEL* expression plasmid. (Right) Cell lysates were subjected to immunoblotting analysis with antibodies against the indicated proteins. α-tubulin was used as a loading control. (d) qRT-PCR analysis of *ASBEL* and *ANA/BTG3* expression in JHOC5 cells infected with a lentivirus expressing an shRNA targeting ANA/BTG3. (e) JHOC5 cells that had been infected with a lentivirus expressing shRNA targeting *ANA/BTG3* was transfected with siRNA targeting *ASBEL* and their viability was assessed. *, $P < 0.05$.

formation with their antisense transcript[5,6,10]. However, *ASBEL* does not affect *ANA/BTG3* mRNA expression but rather regulates the levels of ANA/BTG3 protein. Furthermore, our subcellular fractionation and RT-PCR analyses revealed that *ASBEL* forms duplexes with *ANA/BTG3* mRNA in the nucleus and suppresses its cytoplasmic transportation (Fig. 5). Although some ncRNAs such as the nuclear-retained ncRNA *MALAT1* are known to regulate alternative splicing[22], our results showed that *ASBEL* does not affect splicing of *ANA/BTG3* mRNA. The mechanism by which *ASBEL* inhibits cytoplasmic transportation of *ASBEL-ANA/BTG3* RNA duplexes remains to be elucidated. Investigation of the normal function of *ASBEL* and regulation of its activity is also underway in our laboratories.

Methods

Cell culture. OVISE, JHOC5, JHOC9, OV1063, and 2008 cells were cultured in RPMI1640 supplemented with 10% bovine serum. 293FT cells were cultured in DMEM supplemented with 10% bovine serum.

Antibodies. Anti-FLAG (F3165) antibody was obtained from Sigma. Anti-Lamin A/C (612162) antibody was obtained from BD Biosciences. Anti-α-tubulin (CP-06) antibody was from CALBIOCHEM. Anti-ANA/BTG3 antibody was prepared as described previously[17].

Strand-specific RT-PCR. RNA isolated using TRIsure (BIOLINE) was treated with DNase I (TAKARA), and reverse transcribed using Superscript III (Invitrogen) in the presence of strand-specific primers (2 pmol) (Supplementary Table S1) or oligo(dT) (500 ng) at 55°C. PCR amplification was performed using the indicated primers.

Northern blot. Total RNA was isolated using TRIsure (BIOLINE) and poly(A)+−enriched RNA was purified using Dynabeads Oligo $(dT)_{25}$ magnetic beads (Invitrogen). Poly(A)+−enriched RNA was boiled in formamide loading buffer, separated by gel electrophoresis with a 2% denaturing formaldehyde gel in 1 × MOPS buffer, transferred to Hybond N+ (Amersham) in 20 × SSC (3 M NaCl, 0.3 M Na_3−citrate). Membranes were cross-linked by ultraviolet irradiation and hybridized over-night at 60°C with ^{32}P-dCTP-labelled DNA probes in Hybridization Buffer (7% SDS, 0.5 M Sodium Phosphate, pH7.2, 1 mM EDTA). The membranes were washed with NB Wash Buffer A (1 × SSC, 0.1% SDS) for 10 min at 25°C and then twice with NB Wash Buffer B (2 × SSC, 0.5% SDS) for 20 min at 60°C. Signals were visualized on a phosphorimager (Typhoon FLA 7000, GE Healthcare). DNA probes were labelled with ^{32}P-dCTP using the Megaprime DNA Labelling System (GE Healthcare). Primers used for generating probes are shown in Supplementary Table S2 online.

qRT-PCR analysis. Total RNA was isolated using the Total RNA Isolation kit (MACHEREY-NAGEL) and treated with DNase I (TAKARA). One microgram RNA was reverse transcribed using PrimeScript RT Master Mix (TAKARA, RR036A). qRT-PCR analysis of cDNA was performed on a LightCycler 480 (Roche Applied Science) using Syber Green PCR mastermix (Applied Biosystems). Primers used for qRT-PCR are shown in Supplementary Table S3 online.

Patients and specimens. Tissue samples of eleven ovarian cancers were obtained from the Jikei University hospital, Tokyo. Informed consent was obtained from all patients. This study was approved by the Ethics Committee of the Jikei University and the University of Tokyo. Eleven ovarian cancer samples include 5 serous adenocarcinoma, 2 endometrioid adenocarcinoma, 2 clear cell adenocarcinoma, 1 mucinous adenocarcinoma, and 1 dysgerminoma.

Lentivirus production. Lentiviral vector (CS-Rfa-CG) harbouring an shRNA driven by the H1 promoter was transfected with the packaging vectors pCAG-HIV-gp and pCMV-VSV-G-RSV-Rev into 293FT cells using polyethylenimine 'MAX' (PEI, Polyscience, Inc. Cat. 24765). All plasmids were kindly provided by H. Miyoshi (RIKEN BioResource Center, Japan). Virus supernatants were purified by ultracentrifugation at 25,000 rpm for 90 min (SW28 rotor, Beckman). Infection efficiency was monitored by GFP expression as it is driven by the CMV promoter. The sequences of shRNAs are shown in Supplementary Table S4 online.

RNA interference. Stealth siRNA duplexes targeting ANA/BTG3 were purchased from Invitrogen. siRNA duplexes targeting *ASBEL* were purchased from Exiqon. Cells were transfected with RNA duplexes using Lipofectamine RNAiMAX (Invitrogen). The sequences of siRNAs are shown in Supplementary Table S4 online. Validated Stealth negative control RNAi duplex with MED GC content #2 (Invitrogen) or siRNA negative control (Exiqon, S20C-0600) was used as a control.

Constructs and transfection. An oligonucleotide coding for an RNA hairpin that binds bacteriophage pp7 coat protein[23,24] was cloned as an NheI-HindIII fragment in pcDNA3.1(+) (Invitrogen) [termed pcDNA3.1(+)-pp7-5′]. FLAG tag and the nuclear localization signal from the SV40 large T-antigen was added to the 5′ end of the pp7 coat protein cDNA [a gift form D. S. Peabody (University of New Mexico School of Medicine)] by PCR and cloned into pcDNA3.1(+). *ASBEL*, *ASBEL-Del-1* (1 to 926), *ASBEL-Del-2* (1 to 1178), *ASBEL-Del-3* (927 to 2312), *ASBEL-Del-4* (1179 to 2312) were amplified by PCR using corresponding specific primers and cloned into pcDNA3.1(+)−pp7-5′. A fragment containing the *ANA/BTG3* 5′UTR was amplified by PCR from the JHOC5 genome and was subcloned with the *ANA/BTG3* ORF into pcDNA3.1(+). Primers used for construction are shown in Supplementary Table S5 online. Plasmids were transfected into cells using polyethylenimine 'MAX' (PEI, Polyscience, Inc. Cat. 24765).

Immunoblotting. Cells (5 × 10^6) were lysed for 20 min with lysis buffer (0.5% Triton X-100, 100 mM NaCl, 50 mM Tris-HCl pH7.5, 2 mM EDTA, 50 mM sodium fluoride) containing protease inhibitors. After centrifugation at 23,100 × g for 20 min at 4°C, samples were resolved by SDS-PAGE and then transferred to PVDF membranes (Immobilon-P, Millipore) and analyzed by immunoblotting using HRP-conjugated secondary antibodies. Membranes were blocked with 5% skimmed milk in TBS plus Tween 20 at 4°C overnight before probing with antibodies. Visualization was performed using the Enhanced Chemiluminescence Plus Western Blotting Detection System (GE Healthcare) and LAS-4000EPUVmini Luminescent Image Analyzer (GE Healthcare).

Apoptosis. Phosphatidylserine (PS) exposure at the cell surface was detected using the Annexin V-Biotin Apoptosis Detection Kit (MBL) and Streptavidin–APC conjugates (S888, Invitrogen) according to the manufacture's instruction.

MTT assay. One week after lentivirus infection, cells were treated with C3-(4,5-dimethylthiazol-2-yl)-2,5-diphenyltetrazolium (MTT) (Calbiochem) for 4 h. Cell viability was determined by measuring the absorbance at 570 nm using a

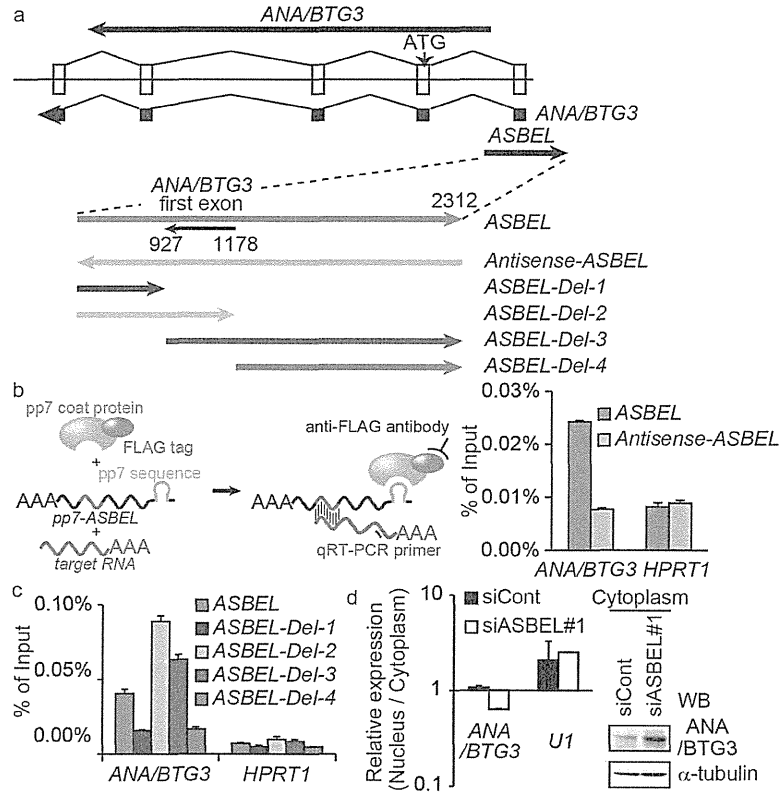

Figure 4 | *ASBEL* forms duplexes with *ANA/BTG3* mRNA and prevents its nuclear-cytoplasmic transportation. (a) Schematic representation of the genomic organization of the region containing *ASBEL* and *ANA/BTG3* and the *ASBEL* mutant constructs used in RIP assays. (b, c) RIP assay. Lysates prepared from JHOC5 cells transfected with the wild type, antisense (*Antisense-ASBEL*) or mutant *pp7-ASBEL* (*ASBEL* fused to a pp7 coat protein-binding sequence), *ANA/BTG3* mRNA and FLAG-tagged pp7 coat protein expression constructs were subjected to immunoprecipitation with anti-FLAG antibody followed by RT-PCR analysis to detect *ANA/BTG3* mRNA. Four mutants shown in (a) were used in (c). The apparent immunoprecipitation efficiency for a specific RNA was calculated by dividing the amount of RT-PCR product obtained in the immunoprecipitated sample by the amount obtained from the input RNA. *HPRT1* was used as a negative control. (d) Subcellular distribution of *ANA/BTG3* mRNA and ANA/BTG3 protein. JHOC5 cells transfected with siRNA targeting *ASBEL* or control siRNA were subjected to subcellular fractionation. (Left) The amounts of the indicated RNAs in each fraction were evaluated by RT-PCR analysis. *U1* was used as a loading control. (Right) The cytoplasmic fraction was subjected to immunoblotting analysis with antibodies against the indicated proteins. α-tubulin was used as a loading control.

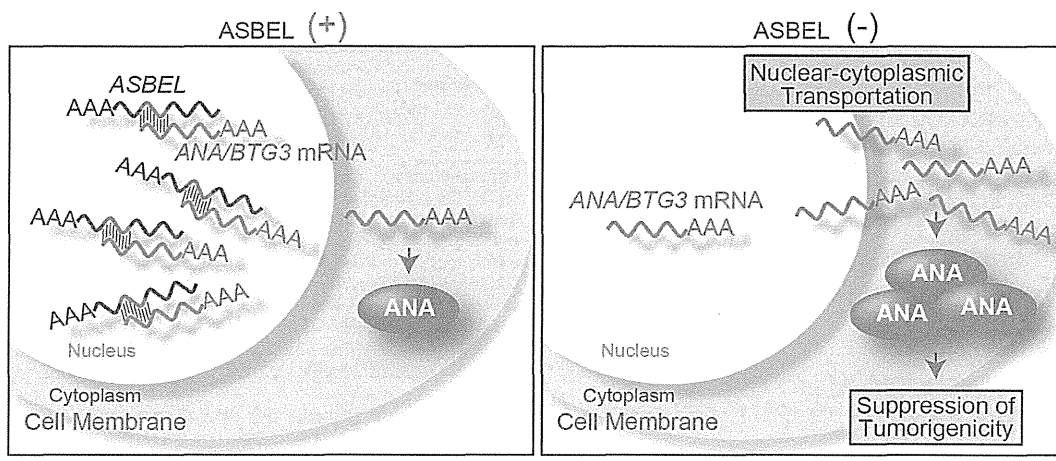

Figure 5 | The ncRNA *ASBEL* is required for tumorigenicity of ovarian cancer. *ASBEL* forms duplexes with *ANA/BTG3* mRNA in the nucleus and suppresses its nuclear-cytoplasmic transportation. *ASBEL*-mediated inhibition of ANA/BTG3 protein expression may be important for the tumorigenicity of ovarian cancer.

Mithras LB 940 (Berthold). The absorbance values of formazan were calculated as a percentage of the control wells.

CellTiter-Glo. Cell viability was determined indirectly by measuring the intracellular levels of ATP using the CellTiter-Glo Luminescent Cell Viability Assay kit (Promega). Luminescence was measured on a Mithras LB 940 (Berthold).

Subcutaneous xenograft. JHOC5 cells infected with a lentivirus expressing an shRNA targeting *ASBEL*were injected stereotactically into 6-week-old nude mice (BALB/cAJcl-*nu/nu*, CLEA Japan). All animal experimental protocols were performed in accordance with the guidelines of the Animal Ethics Committee of the University of Tokyo.

RIP assay. Cells growing in 6-well dishes were lysed in 0.5 ml of 0.5% Lysis buffer (50 mM HEPES pH7.5, 150 mM KCl, 0.5% NP40, 2 mM EDTA, 1 mM NaF) containing protease inhibitors and RNase Inhibitor (Promega), and centrifuged at 13,000 r.p.m. for 10 min. The supernatant were incubated with anti-FLAG antibody for 3 h at 4°C with gentle rotation. Thirty microliters of Protein G Dynabeads (Invitrogen) were added and then incubated for 1 h at 4°C with gentle rotation. The beads were washed thrice with Wash buffer (50 mM HEPES pH7.5, 150 mM KCl, 0.05% NP40) containing RNase Inhibitor (Promega) and then twice with PBS containing RNase Inhibitor (Promega). RNA was extracted using the Total RNA Isolation kit (MACHEREY-NAGEL) and qRT-PCR was performed as described above. Primers for qRT-PCR are shown in Supplementary Table S3 online.

Subcellular fractionation. Cells were washed and harvested in PBS. The pellet was resuspended in 1 packed cell volume of Hypotonic Buffer (10 mM HEPES pH 7.5, 10 mM KCl, 1.5 mM $MgCl_2$). After incubation on ice for 10 min, cells were disrupted by 10 passages through a 25-gauge needle. Cells were centrifuged for 10 min at 1,000 g at 4°C and the supernatant containing the cytoplasmic fraction was collected by further centrifugation at 17,000 g for 15 min. The remaining pellet was washed twice with Hypotonic Buffer, resuspended in Hypertonic Buffer (20 mM HEPES pH 7.5, 420 mM KCl, 1.5 mM $MgCl_2$, 0.5% NP40) and incubated at 4°C for 30 min with gentle rotation. The supernatant containing the nuclear fraction was collected by centrifugation at 18,000 g for 15 min.

Polysome preparation. The JHOC5 cytoplasmic fraction in hypotonic buffer (10 mM HEPES pH 7.5, 10 mM KCl, 1.5 mM $MgCl_2$, 150 μg/mL cycloheximide) was layered onto a 10mL linear sucrose gradient (10%-55% sucrose, 50 mM Tris-HCl pH7.5, 75 mM KCl, 1.5 mM $MgCl_2$, 0.5 mM DTT) containing protease inhibitors and RNase Inhibitor (Promega), and centrifuged in a SW40Ti rotor (Beckman) for 15 h at 25,000 rpm at 4°C. Fractions were collected with a Piston Gradient Fractionator (Biocomp). RNA was extracted using the Total RNA Isolation kit (MACHEREY-NAGEL).

1. Katayama, S. *et al.* Antisense transcription in the mamalian transcriptome. *Science* **309**, 1564–1566 (2005).
2. Faghihi, M. A. & Wahlestedt, C. Regulatory roles of natural antisense transcripts. *Nat. Rev. Mol. Cell Biol.* **10**, 637–643 (2009).
3. Hastings, M. L., Milcarek, C., Martincic, K., Peterson, M. L. & Munroe, S. H. Expression of the thyroid hormone receptor gene, erbAalpha, in B lymphocytes: alternative mRNA processing is independent of differentiation but correlates with antisense RNA levels. *Nucleic Acids Res.* **25**, 4296–4300 (1997).
4. Peters, N. T., Rohrbach, J. A., Zalewski, B. A., Byrkett, C. M. & Vaughn, J. C. RNA editing and regulation of Drosophila 4f-rnp expression by sas-10 antisense readthrough mRNA transcripts. *RNA* **9**, 698–710 (2003).
5. Faghihi, M. A. *et al.* Expression of a noncoding RNA is elevated in Alzheimer's disease and drives rapid feed-forward regulation of beta-secretase. *Nat. Med.* **14**, 723–730 (2008).
6. Matsui, K. *et al.* Natural antisense transcript stabilizes inducible nitric oxide synthase messenger RNA in rat hepatocytes. *Hepatology* **47**, 686–697 (2008).
7. Uchida, T. *et al.* Prolonged hypoxia differentially regulates hypoxia-inducible factor (HIF)-1alpha and HIF-2alpha expression in lung epithelial cells: implication of natural antisense HIF-1alpha. *J. Biol. Chem.* **279**, 14871–14878 (2004).
8. Hatzoglou, A. *et al.* Natural antisense RNA inhibits the expression of BCMA, a tumour necrosis factor receptor homologue. *BMC Mol. Biol.* **3**, 4 (2002).
9. Ebralidze, A. K. *et al.* PU.1 expression is modulated by the balance of functional sense and antisense RNAs regulated by a shared cis-regulatory element. *Genes Dev.* **22**, 2085–2092 (2008).
10. Mahmoudi, S. *et al.* Wrap53, a natural p53 antisense transcript required for p53 induction upon DNA damage. *Mol. Cell* **33**, 462–471 (2009).
11. Tufarelli, C. *et al.* Transcription of antisense RNA leading to gene silencing and methylation as a novel cause of human genetic disease. *Nat. Genet.* **34**, 157–165 (2003).
12. Yu, W. *et al.* Epigenetic silencing of tumour suppressor gene p15 by its antisense RNA. *Nature* **451**, 202–206 (2008).
13. Morris, K. V., Santoso, S., Turner, A. M., Pastori, C. & Hawkins, P. G. Bidirectional transcription directs both transcriptional gene activation and suppression in human cells. *PLoS Genet.* **4**, e1000258 (2008).
14. Winkler, G. S. The mammalian anti-proliferative BTG/Tob protein family. *J. Cell. Phys.* **222**, 66–72 (2010).
15. Lin, T. Y. *et al.* Loss of the candidate tumor suppressor BTG3 triggers acute cellular senescence via the ERK-JMJD3-p16(INK4a) signaling axis. *Oncogene* **31**, 3287–3297 (2012).
16. Ou, Y. H. *et al.* The candidate tumor suppressor BTG3 is a transcriptional target of p53 that inhibits E2F1. *EMBO J.* **26**, 3968–3980 (2007).
17. Yoshida, Y., Hosoda, E., Nakamura, T. & Yamamoto, T. Association of ANA, a member of the antiproliferative Tob family proteins, with a Caf1 component of the CCR4 transcriptional regulatory complex. *Jan. J. Cancer Res.* **92**, 592–596 (2001).
18. Majid, S. *et al.* BTG3 tumor suppressor gene promoter demethylation, histone modification and cell cycle arrest by genistein in renal cancer. *Carcinogenesis* **30**, 662–670 (2009).
19. Yoneda, M. *et al.* Deficiency of antiproliferative family protein Ana correlates with development of lung adenocarcinoma. *Cancer Sci.* **100**, 225–232 (2009).
20. Mahmoudi, S. *et al.* Wrap53, a natural p53 antisense transcript required for p53 induction upon DNA damage. *Mol. Cell* **33**, 462–471 (2009).
21. Dallosso, A. R. *et al.* Alternately spliced WT1 antisense transcripts interact with WT1 sense RNA and show epigenetic and splicing defects in cancer. *RNA* **13**, 2287–2299 (2007).
22. Tripathi, V. *et al.* The nuclear-retained noncoding RNA MALAT1 regulates alternative splicing by modulating SR splicing factor phosphorylation. *Mol. Cell* **39**, 925–938 (2010).
23. Lim, F. & Peabody, D. S. RNA recognition site of PP7 coat protein. *Nucleic Acids Res.* **30**, 4138–4144 (2002).
24. Lim, F., Downey, T. P. & Peabody, D. S. Translational repression and specific RNA binding by the coat protein of the Pseudomonas phage PP7. *J. Biol. Chem.* **276**, 22507–22513 (2001).

Ackowledgements

This work was supported by Research Program of Innovative Cell Biology by Innovative Technology (Integrated Systems Analysis of Cellular Oncogenic Signaling Networks), Grants-in-Aid for Scientific Research on Innovative Areas (Integrative Research on Cancer Microenvironment Network), Project for Development of Innovative Research on Cancer Therapeutics, Takeda Science Foundation and in part by Global COE Program (Integrative Life Science Based on the Study of Biosignaling Mechanisms), MEXT, Japan.

Author contributions

S.Y., K.T., A.O. and T.A. conceived the project and designed the experiments. S.Y. and K.T. performed most of the experiments. H.S., E.N., Y.T., M.K., K.O. generated some expression constructs and performed RT-PCR analyses. T.Y. prepared anti-ANA/BTG3 antibody. S.Y. and A.O. prepared ovarian cancer specimens. S.Y., K.T., A.O. and T.A. wrote the manuscript.

Additional information

Supplementary information accompanies this paper at http://www.nature.com/scientificreports

Competing financial interests: The authors declare no competing financial interests.

License: This work is licensed under a Creative Commons Attribution-NonCommercial-NoDerivs 3.0 Unported License. To view a copy of this license, visit http://creativecommons.org/licenses/by-nc-nd/3.0/

How to cite this article: Yanagida, S. *et al.* ASBEL, an ANA/BTG3 antisense transcript required for tumorigenicity of ovarian carcinoma. *Sci. Rep.* 3, 1305; DOI:10.1038/srep01305 (2013).